

## Journal Pre-proofs

Ammonia recovery from acidogenic fermentation effluents using a gas-permeable membrane contactor

A. Serra-Toro, S. Vinardell, S. Astals, S. Madurga, J. Llorens, J. Mata-Álvarez, F. Mas, J. Dosta

PII: S0960-8524(22)00602-2  
DOI: <https://doi.org/10.1016/j.biortech.2022.127273>  
Reference: BITE 127273

To appear in: *Bioresource Technology*

Received Date: 14 March 2022  
Revised Date: 30 April 2022  
Accepted Date: 2 May 2022

Please cite this article as: Serra-Toro, A., Vinardell, S., Astals, S., Madurga, S., Llorens, J., Mata-Álvarez, J., Mas, F., Dosta, J., Ammonia recovery from acidogenic fermentation effluents using a gas-permeable membrane contactor, *Bioresource Technology* (2022), doi: <https://doi.org/10.1016/j.biortech.2022.127273>

This is a PDF file of an article that has undergone enhancements after acceptance, such as the addition of a cover page and metadata, and formatting for readability, but it is not yet the definitive version of record. This version will undergo additional copyediting, typesetting and review before it is published in its final form, but we are providing this version to give early visibility of the article. Please note that, during the production process, errors may be discovered which could affect the content, and all legal disclaimers that apply to the journal pertain.

© 2022 Published by Elsevier Ltd.



1 **Ammonia recovery from acidogenic fermentation effluents using a gas-**  
2 **permeable membrane contactor**

3 A. Serra-Toro<sup>1</sup>, S. Vinardell<sup>1</sup>, S. Astals<sup>1</sup>, S. Madurga<sup>2</sup>, J. Llorens<sup>1</sup>, J. Mata-Álvarez<sup>1,3</sup>, F.

4 Mas<sup>2</sup>, J. Dosta<sup>1,3\*</sup>

5 <sup>1</sup> Chemical Engineering and Analytical Chemistry Department. University of Barcelona,

6 Barcelona, Catalonia, Spain

7 <sup>2</sup> Materials Science and Physical Chemistry Department & Research Institute of

8 Theoretical and Computational Chemistry (IQTCUB), University of Barcelona,

9 Barcelona, Catalonia, Spain

10 <sup>3</sup> Water Research Institute, University of Barcelona, Barcelona, Catalonia, Spain

11 \* Corresponding author: jdosta@ub.edu

12 **Abstract**

13 A gas-permeable membrane (GPM) contactor was used to recover ammoniacal  
14 nitrogen from a synthetic and a biowaste fermentation broth under different pH (from  
15 6 to 11) and temperatures (35 and 55 °C). Ammonia mass transfer constant ( $K_m$ )  
16 increased as pH and temperature increased. For synthetic broth, pH 10 provided the  
17 best results, when considering the  $K_m$  ( $9.2 \cdot 10^{-7} \text{ m} \cdot \text{s}^{-1}$ ) and the reagents consumption  
18 ( $1.0 \text{ mol NaOH mol}^{-1} \text{ TAN}$  and  $1.2 \text{ mol H}_2\text{SO}_4 \cdot \text{mol}^{-1} \text{ TAN}$ ). Biowaste fermentation  
19 generated a broth with a high concentration of ammoniacal nitrogen ( $4.9 \text{ g N} \cdot \text{L}^{-1}$ ) and  
20 volatile fatty acids (VFA) ( $28.5 \text{ g} \cdot \text{L}^{-1}$ ). Experiments using the biowaste broth showed a

21 lower  $K_m$  ( $5.0 \cdot 10^{-7} \text{ m} \cdot \text{s}^{-1}$  at pH 10) than the synthetic broth, related to the solution  
22 matrix and other species interference. VFAs were not detected in the trapping  
23 solution. Overall, these results show that GPM is a suitable technology to efficiently  
24 separate ammoniacal nitrogen and VFA from fermentation broths.

25 **KEYWORDS:** membrane technology; nitrogen recovery; food waste fermentation;  
26 volatile fatty acids; biorefinery

## 27 1. Introduction

28 Gas-permeable membrane (GPM) contactor is an emerging technology to recover  
29 ammoniacal nitrogen from wastewater as N-based fertiliser (e.g.  $(\text{NH}_4)_2\text{SO}_4$ ,  $\text{NH}_4\text{NO}_3$ ,  
30  $(\text{NH}_4)_2\text{HPO}_4$ ), with a market value of 0.4-1.0  $\text{€} \cdot \text{kg}^{-1}$  N for  $(\text{NH}_4)_2\text{SO}_4$  (Darestani et al.,  
31 2017; Menkveld and Broeders, 2018). In GPM, ammonia ( $\text{NH}_3$ ) diffuses across the  
32 membrane from the feed-membrane interface to an acidic trapping solution.  $\text{NH}_3$  is a  
33 non-charged species able to diffuse through a nano-perforated hydrophobic  
34 membrane, and its diffusion is driven by the  $\text{NH}_3$  concentration difference between the  
35 feed and the trapping solution. Once at the acidic solution,  $\text{NH}_3$  is protonated and  
36 converted to ammonium ( $\text{NH}_4^+$ ), an ionised species unable to diffuse across the  
37 membrane. Liquid penetration into the pores (membrane wetting) is prevented by (i)  
38 the hydrophobic nature of the membrane and (ii) the small size of the nanopores due  
39 to the capillary effect (Boehler et al., 2015).

40 GPM contactors have been successfully used to recover total ammoniacal nitrogen  
41 (TAN) from anaerobic digestion supernatants (Noriega-Hevia et al., 2020; Dube et al.,  
42 2016), the effluent of a primary treatment in a municipal wastewater treatment plant

43 (Lee et al., 2021), concentrates from the regeneration of zeolites (Vecino et al., 2019),  
44 human urine (Nagy et al., 2019), and pig slurry (García-González and Vanotti, 2015;  
45 García-González et al., 2015; Riaño et al., 2019). However, the recovery of TAN from  
46 fermentation broths has not been reported, despite the potential application of this  
47 approach in biorefineries schemes that require to decouple easily biodegradable  
48 organic matter from TAN. This would be the case of the proposed biorefinery scheme  
49 that aims to produce polyhydroxyalkanoates (PHA) from biowaste (Figure 1).  
50 PHA production using mixed-cultures is typically carried out by a 3-stage process (Reis  
51 et al, 2011; Frison et al., 2015). In the anaerobic stage, the biowaste is fermented to  
52 produce a volatile fatty acids (VFA) rich fermentation broth. In the selection stage, a  
53 sequencing batch reactor fed with the fermentation liquid (liquid fraction from  
54 fermentation broth solid-liquid separation) produces biomass with high PHA storage  
55 capacity by alternating periods with high VFA availability (feast) and periods with  
56 absence of VFA (famine). In the accumulation stage, the selected PHA-storing biomass  
57 is fed with the VFA-rich fermentation liquid (batch mode and aerobic conditions) to  
58 promote the maximum accumulation of PHA. Recovering TAN from the fermentation  
59 liquid before using it as carbon source in the selection reactor could enhance the  
60 efficiency of PHA production by decoupling the carbon and nitrogen availability in the  
61 feast and famine phases. Oliveira et al. (2017), Silva et al. (2017) and Lorini et al. (2020)  
62 improved PHA production when carbon and nitrogen were fed separately.

63 Recovering nitrogen from the fermentation liquid with GPM would also reduce the  
64 TAN concentration in the anaerobic digester that treats the unfermented solid fraction  
65 and other reject streams of the biorefinery (Figure 1). This feature could alleviate or

66 avoid  $\text{NH}_3$  inhibition of the anaerobic digestion process (Capson-Tojo et al. 2020). In  
67 this regard, Lauterböck et al. (2014) reported an improved methane production from  
68 slaughterhouse wastewater when the TAN concentration was decreased from 6.5 to  
69  $2.5 \text{ g TAN}\cdot\text{L}^{-1}$  in the anaerobic digester. Shi et al. (2019) achieved a stable operation at  
70 high organic loading rates in an anaerobic digester treating food waste after TAN  
71 recovery. Bayrakdar et al. (2017) and González-García et al. (2021) also reported a  
72 positive impact on the biogas production in an anaerobic digester treating chicken and  
73 pig manure, respectively.

74 Several factors influence TAN recovery by GPM such as pH, temperature, salinity, initial  
75 TAN concentration, the feed flowrate, the membrane material and contactor  
76 configuration, and membrane fouling (Boehler et al., 2015; Rongwong and Goh, 2020).  
77 Among them, pH and temperature are particularly important since they have a  
78 noticeable impact on  $\text{NH}_4^+/\text{NH}_3$  equilibrium. Many studies have evaluated the impact  
79 of pH and temperature on the efficiency of GPM contactors (Fillingham et al., 2017;  
80 Noriega-Hevia et al., 2020). However, to the best of the authors' knowledge, the  
81 impact of pH and temperature on GPM performance has not yet been evaluated for a  
82 hybrid process recovering TAN from fermentation broths. This is an important  
83 application because fermentation and GPM could be important technologies in future  
84 biorefineries. Accordingly, an experimental study evaluating the impact of pH and  
85 temperature on the performance of GPM is important to understand how these two  
86 operational factors influence the recovery of TAN from fermentation broths.  
87 This work assesses the impact of pH and temperature on the performance of a GPM  
88 contactor to separate TAN and VFAs from biowaste fermentation broths. The recovery

89 of TAN was evaluated for a synthetic and a biowaste fermentation liquid under  
90 different pH and temperature conditions. The ultimate goal was to find the optimum  
91 pH and temperature condition to integrate a hybrid GPM process that recovers TAN as  
92 N-based fertiliser and produces a VFA-rich stream with limited N concentration from  
93 fermentation broths.

## 94 2. Material and methods

### 95 2.1 Synthetic solution and OFMSW

96 Synthetic and organic fraction of municipal solid waste (OFMSW) fermentation broths  
97 were used in this study. The synthetic broth consisted in deionised water containing  
98  $7.0 \text{ g NH}_4\text{Cl}\cdot\text{L}^{-1}$  ( $2.35 \text{ g TAN}\cdot\text{L}^{-1}$ ) and  $3.0 \text{ g}\cdot\text{L}^{-1}$  of acetic acid ( $3.2 \text{ g COD}\cdot\text{L}^{-1}$ ). Acetic acid  
99 was selected to determine the maximum diffusion of VFA through the membrane since  
100 this is the VFA with the lowest molecular weight. The OFMSW fermentation broth was  
101 obtained from OFMSW fermentation at  $35 \text{ }^\circ\text{C}$  (see characterisation in e-supplementary  
102 material). The OFMSW was collected from a mechanical-biological treatment (MBT)  
103 plant of the Barcelona Metropolitan Area (Spain) that treats about 50,000 t per year of  
104 source-sorted OFMSW. The OFMSW was collected after the pre-treatment and before  
105 its feeding to the anaerobic digesters (see description of the MBT plant in Fernández-  
106 Domínguez et al., 2020). The high soluble COD and VFA concentration of the collected  
107 OFMSW could be attributed to the pre-fermentation of the OFMSW in the pulper and  
108 hydrocyclones system of the MBT plant.

### 109 2.2 Experimental set-up

#### 110 2.2.1 Acidogenic fermenter

111 A 40-L fermenter at mesophilic conditions (35 °C) was used to produce the OFMSW  
112 fermentation broth. The fermenter was equipped with a mechanical stirrer (Triam,  
113 75040), a pH probe system (Crison pH 28), a heating system (AS, Electric Heating  
114 Jacket) and an alleviation valve located at the top of the fermenter to avoid  
115 overpressure. 30 kg of OFMSW were fed to the reactor without adding external  
116 inoculum nor external chemicals since it was considered that the anaerobic digestion  
117 supernatant recirculation provided enough fermentative bacteria and alkalinity. The  
118 fermentation batch lasted 8 days, when the VFA concentration reached its maximum  
119 value. The fermentation broth used in the membrane contactor was obtained after  
120 sieving (0.05 mm mesh size), centrifuging (16600 × g, 10 min) and filtering (1.2 µm  
121 mesh light filter) the fermentation broth. The resulting fermentation liquid was stored  
122 at 4 °C until use.

### 123 **2.2.2. Membrane contactor**

124 Figure 2 shows the membrane contactor experimental set-up used to recover TAN  
125 from the feed solution. Two 2-L jacketed glass tanks were used as chambers for the  
126 feed (fermentation broth) and the acidic trapping solution (initial solution of 0.1 M  
127 H<sub>2</sub>SO<sub>4</sub>). The feed and trapping solutions were pumped using a peristaltic pump in a  
128 closed loop to a microporous hollow-fibre polypropylene (PP) membrane contactor  
129 with an active surface area of 0.50 m<sup>2</sup> (3M, 1.7 x 5.5 MiniModule). The relation  
130 between feed solution and trapping solution flow rates was 3:1 according to  
131 manufacturer's recommendations. Specifically, the feed solution flow rate was 15 L·h<sup>-1</sup>  
132 (shell side of the membrane) and the trapping solution flow rate was 5 L·h<sup>-1</sup> (lumen  
133 side of the contactor). The operational temperature was achieved by circulating water

134 from a heated water bath through a jacket surrounding the tanks. These tanks were  
135 sealed to minimise  $\text{NH}_3$  losses by volatilisation. Each tank was equipped with a  
136 magnetic stirrer (180 rpm) and a pH control system consisting of a pH electrode  
137 (Crison, code 53 35) and a pH controller (Crison, pH 28), connected to peristaltic  
138 pumps (Ismatec, Type ISM827). The peristaltic pumps dosed an acid solution ( $\text{H}_2\text{SO}_4$   
139 75%) to keep the trapping solution at pH 1.0 and an alkali solution (NaOH 10 M) to  
140 keep the feed solution at the targeted set point. The trapping solution needs to be acid  
141 enough to retain the  $\text{NH}_3$  diffused from the feed solution as  $\text{NH}_4^+$ , since charged  
142 species are not able to diffuse through the membrane. The feed solution needs to be  
143 alkaline to displace the TAN equilibrium towards  $\text{NH}_3$ , which is the non-charged species  
144 able to diffuse across the membrane from the feed to the trapping solution. The  
145 fermentation liquor was filtered through 1.2  $\mu\text{m}$  filters to prevent membrane clogging.

### 146 2.3 Membrane contactor operational conditions

147 Table 1 summarizes the operational conditions of the experiments carried out with the  
148 membrane contactor. Firstly, the effect of pH (6.0, 7.0, 8.0, 9.0, 10.0 and 11.0) and  
149 temperature (35 and 55 °C) was evaluated using the synthetic fermentation liquid as a  
150 feed solution. These temperatures were selected since both mesophilic (35 °C) and  
151 thermophilic (55 °C) conditions are used to ferment OFMSW (Bolzonella et al., 2012;  
152 Micolucci et al., 2020; Valentino et al., 2021). Subsequently, considering the results  
153 from the synthetic fermentation liquid, experiments at pH of 9.0 and 10.0 and at  
154 temperature of 35 and 55 °C were carried out using the OFMSW fermentation liquid as  
155 feed solution. The experiments carried out with the synthetic fermentation liquid had  
156 2 L of feed and trapping solution, while the experiments using the OFMSW



157 fermentation liquid were conducted with a lower volume (0.5 L of feed and trapping  
158 solutions) due to the difficulty to filter the OFMW fermentation broth through 1.2  $\mu\text{m}$   
159 filters. All conditions were tested by duplicate.

160 The process was monitored by withdrawing several samples from the feed and  
161 trapping solution during the experiments (ca. 8 hours). The sampling frequency was  
162 once per hour, except the first hour where two samples were withdrawn. In each  
163 sampling event, 4 mL were withdrawn from both solutions. For the feed solution  
164 sample, 0.1 mL of sulfuric acid (1 M) was immediately added to decrease the pH and  
165 prevent TAN losses by volatilisation. All samples were stored at 4 °C prior analysis.

166 The TAN recovery efficiency was calculated using Equation 1, where  $\text{TAN}_f(0)$  is the  
167 initial TAN mass in the feed solution (g),  $\text{TAN}_t(0)$  is the initial TAN mass in the trapping  
168 solution (g), and  $\text{TAN}_t(t)$  is the TAN mass at a specific time (g). The nitrogen mass  
169 balance showed that nitrogen losses by volatilisation were minimal (< 1%).  
170 Accordingly, it was assumed that there were no losses of  $\text{NH}_3$  by volatilisation.

$$171 \quad \% \text{ TAN recovery } (t) = \frac{\text{g TAN}_t(t) - \text{g TAN}_t(0)}{\text{g TAN}_f(0)} \cdot 100 \quad (1)$$

## 172 **2.4 Analytical methods**

173 All the analyses were performed according to the Standard Methods for the  
174 Examination of Water and Wastewater (APHA, 2017). TAN concentration was  
175 determined using a Thermo Fisher Scientific ion-selective electrode (Orion  
176 9512HPBNWP) following the procedure 4500-NH3D. Total solids (TS) and volatile solids  
177 (VS) were measured according to Standard Method 2540G (APHA, 2017). Alkalinity was  
178 determined following the Standard Method 2320B, using an automated titrator (Crison

179 pH Burette 24) with a 0.1 M HCl solution and a pH endpoint of 4.30. The soluble  
180 fraction was obtained by centrifuging the samples at  $16600 \times g$  (Sigma 1-14  
181 microcentrifuge) for 10 min and filtering the supernatant through a  $1.2 \mu\text{m}$  mesh light  
182 cellulose filter. Soluble COD was determined according to the Standard Method 5220C  
183 (APHA, 2017). Cations ( $\text{Li}^+$ ,  $\text{Na}^+$ ,  $\text{K}^+$ ,  $\text{Ca}^{2+}$ ,  $\text{Mg}^{2+}$ ) and anions ( $\text{F}^-$ ,  $\text{Cl}^-$ ,  $\text{NO}_2^-$ ,  $\text{Br}^-$ ,  $\text{NO}_3^-$ ,  $\text{SO}_4^{2-}$ ,  
184  $\text{P-PO}_4^{3-}$ ) were analysed using an 863 Advanced Compact IC Metrohm ionic  
185 chromatographer and Metrosep columns (Metrosep C 4-150/4.0 and Metrosep A Supp  
186 17-250/4.0, respectively). VFAs (i.e. acetic, propionic, i-butyric, n-butyric, ivaleric, n-  
187 valeric, i-caproic, n-caproic and heptanoic acid) were analysed using a Shimadzu GC-  
188 2010 plus gas chromatograph equipped with a Nukol™ capillary column and flame  
189 ionisation detector. VFAs were converted to COD equivalents using the theoretical  
190 value ( $\text{mg COD} \cdot \text{mg}^{-1}$  compound): 1.07 for acetic acid, 1.51 for propionic acid, 1.82 for  
191 butyric acid, 2.04 for valeric acid, 2.21 for caproic acid, and 2.34 for heptanoic acid.

## 192 **2.5 Ammonia mass transfer constant assessment**

193  $\text{NH}_3$  flux through the membrane contactor was evaluated by the  $\text{NH}_3$  mass transfer  
194 constant ( $K_m$ ).  $K_m$  is also defined as the conditional permeability of the  $\text{NH}_3$  through the  
195 membrane and allows quantifying the nitrogen transfer under specific conditions  
196 (Ashrafizadez and Khorasani, 2010; Ahn et al., 2011; Reig et al., 2021).

197 The physicochemical model used to determine  $K_m$  considers that: (i) the hydrophobic  
198 membrane is only permeable to  $\text{NH}_3$ , (ii) the pH of the feed and trapping solutions is  
199 constant, (iii) the acid-base equilibrium is always fulfilled at both sides of the

200 membrane, (iv)  $\text{NH}_3$  losses by volatilisation are negligible and (v) the volumes of the  
 201 feed solution ( $V_f$ ) and the trapping solution ( $V_t$ ) are constant.

202  $\text{NH}_3$  transport is described by Fick's law (Equation 2) that considers (i) a behaviour of  
 203 ideal diluted solution for  $\text{NH}_3$  and (ii) no interferences amongst solution components.

$$204 \quad J_{\text{NH}_3,f}(t) = -K_m(c_{\text{NH}_3,t}(t) - c_{\text{NH}_3,f}(t)) \quad (2)$$

205 Where  $J_{\text{NH}_3,f}(t)$  is the flux of  $\text{NH}_3$  ( $\text{mol}\cdot\text{m}^{-2}\cdot\text{s}^{-1}$ ) from the feed to the trapping solution  
 206 (at time  $t$ ),  $K_m$  ( $K_m = D_{\text{NH}_3}/\Delta x$ ) is the  $\text{NH}_3$  mass transfer constant through the  
 207 membrane ( $\text{m}\cdot\text{s}^{-1}$ ),  $D_{\text{NH}_3}$  is the diffusion coefficient of  $\text{NH}_3$  ( $\text{m}^2\cdot\text{s}^{-1}$ ),  $\Delta x$  is the thickness  
 208 of the membrane ( $\text{m}$ ),  $c_{\text{NH}_3,f}(t)$  is the concentration of  $\text{NH}_3$  in the feed solution ( $\text{mol}\cdot\text{m}^{-3}$ ,  
 209 <sup>3</sup>, at time  $t$ ) and  $c_{\text{NH}_3,t}(t)$  is the concentration of  $\text{NH}_3$  in the trapping solution ( $\text{mol}\cdot\text{m}^{-3}$ ,  
 210 at time  $t$ ).

211 The equilibrium reaction  $\text{NH}_4^+ \leftrightarrow \text{NH}_3 + \text{H}^+$ , is described by the following acid-base  
 212 approximate equilibrium constant  $K_a(T)$ , in each side of the membrane,  $i$ :

$$213 \quad K_a(T) \approx \frac{c_{\text{NH}_3,i} \cdot 10^{-\text{pH}_i}}{\gamma_{\text{NH}_4^+,i} \cdot c_{\text{NH}_4^+,i}} \quad (3)$$

214 Where  $\gamma_{\text{NH}_4^+,i}$  is the activity coefficient for  $\text{NH}_4^+$ , which could be described by the  
 215 Davies correction of Debye-Hückel law and depends on the ionic force (assumed to  
 216 remain constant in both sides of the membrane during the process). Equation 4  
 217 correlates the value of  $K_a(T)$  for a given temperature ( $T$ , K) (Anthonisen et al., 1976).

$$218 \quad K_a(T) = e^{-6344/T} \quad (4)$$

219 The TAN mass balance (TAN = NH<sub>3</sub> + NH<sub>4</sub><sup>+</sup>) expressed in terms of the TAN fraction at time

220  $t$  is kept constant:  $z_f(t) + z_t(t) = 1$ , where  $z_i(t) = x_i(t) + y_i(t)$ , and  $x_i(t) = \frac{\text{mol}_{\text{NH}_3,i}(t)}{\text{mol}_{\text{TAN},0}}$ ,

221  $y_i(t) = \frac{\text{mol}_{\text{NH}_4^+,i}(t)}{\text{mol}_{\text{TAN},0}}$ . These are the non-dimensional fractions for both NH<sub>3</sub> and NH<sub>4</sub><sup>+</sup> in

222 terms of the initial TAN.

223 Then, mass transport equation (Equation 2) can be written as Equation 5, which can be

224 arranged in terms of non-dimensional TAN fraction (Equation 6).

$$225 J_{\text{NH}_3,f}(t) = -\frac{1}{A} \left( \frac{d\text{mol}_{\text{NH}_3,f}}{dt} \right) = -K_m \left( \frac{\text{mol}_{\text{NH}_3,t}}{V_t} - \frac{\text{mol}_{\text{NH}_3,f}}{V_f} \right) \quad (5)$$

$$226 \frac{dz_f(t)}{dt} = \alpha (\omega \beta - (1 + \omega \beta) z_f(t)) \quad (6)$$

$$227 \text{Where } \alpha \equiv \frac{K_m A}{V_f}, \omega \equiv \frac{V_f}{V_t}, \beta \equiv \frac{\beta_t}{\beta_f}, \beta_i \equiv \frac{\bar{K}_i}{1 + \bar{K}_i}, \bar{K}_i \equiv \gamma_{\text{NH}_4^+,i} 10^{pH_t - pKa}$$

228 With the initial solution  $z_f(0) = 1$ , the solution of this ordinary differential equation is:

$$229 z_f(t) = \frac{(\omega \beta + \exp(-\alpha(1 + \omega \beta)t))}{1 + \omega \beta} \quad (7)$$

230 With limit solutions that depends on  $\omega$  and  $\beta$ :  $\lim_{t \rightarrow \infty} z_f(t) = \frac{\omega \beta}{1 + \omega \beta}$  and  $\lim_{t \rightarrow \infty} z_t(t) = \frac{1}{1 + \omega \beta}$

231 As  $\beta$  depends on  $pH_t, pH_f, pKa$ , an approximate solution can be derived depending on

232 the trapping solution pH. When the pH of the trapping solution is 1:  $pH_t \ll pKa$ ,  $\bar{K}_t \equiv$

233  $\gamma_{\text{NH}_4^+,t} 10^{pH_t - pKa} \approx \gamma_{\text{NH}_4^+,t} 10^{-8} \ll 1$ , then  $\bar{K}_t \rightarrow 0$ , and  $\beta \rightarrow 0$ . Therefore, Equation 8

234 could be simplified to Equation 8.

$$235 z_f(t) = \exp(-\alpha t) \quad (8)$$

236 A complete recovery of TAN could be reached for operation times long enough ( $\lim_{t \rightarrow \infty} z_f(t)$   
 237  $= 0$ ). Then, Equation 8 in terms of TAN concentration can be written as Equation 9, a  
 238 well-known equation to describe TAN recovery in GPM studies.

$$239 \quad \frac{C_{TAN,f}(t)}{C_{TAN,f}(0)} = \exp\left(-\frac{K_m A}{V_f} t\right) \quad (9)$$

240 This model was coded in Python using the curve fit function of the SciPy. Optimize  
 241 library, which uses the Levenberg-Marquardt algorithm to perform non-linear least  
 242 squares estimates. The algorithm estimates  $K_m$  by fitting the TAN concentration of the  
 243 feed and trapping solution in the tanks over time.

### 244 3. Results and discussion

#### 245 3.1 Ammonia recovery from the synthetic fermentation liquid

246 Figure 3 illustrates the TAN concentration evolution of the experiments carried out  
 247 with synthetic fermentation liquid and Table 2 summarises their performance  
 248 parameters. Experimental results show that the performance (i.e., TAN recovery rate,  
 249 flux,  $K_m$ ) of the membrane contactor improves as the pH of the feed solution increases  
 250 from 6.0 to 11.0. At pH 10.0 and 11.0, TAN was completely recovered after 4 hours of  
 251 experiment at both temperatures, while at pH 6.0 the percentage of TAN recovery was  
 252 lower than 10% after 8 hours. The greater performance of the membrane at higher pH  
 253 can be directly related to the higher amount of  $\text{NH}_3$  in the solution due to the  
 254 displacement of the  $\text{NH}_4^+/\text{NH}_3$  equilibrium (Equation 3). pH values higher than the pKa  
 255 (8.94 and 8.45 at 35 and 55 °C, respectively) implies that the percentage of  $\text{NH}_3$   
 256 represents more than the 50% of the TAN. The process performance was better at 55

257 °C than at 35 °C. However, at pH of 10.0 and 11.0, no statistical difference was  
258 observed between tests carried out at 35 and 55 °C. These results can be explained by  
259 the minimal difference on  $\text{NH}_3$  concentration between pH 10.0 and 11.0 (far above the  
260 pKa). The improved membrane performance at 55 °C can be attributed to the lower  
261 pKa values at higher temperatures, which increases the  $\text{NH}_3$  concentration and the  
262 driving force through the GPM. Besides changes in the pKa value, temperature can also  
263 affect the  $K_m$  since it can modify the membrane properties with a slight impact on  $\text{NH}_3$   
264 diffusivity.

265 TAN flux across the membrane was enhanced as the pH and temperature of the feed  
266 solution increased (Table 2). At 35 °C, increasing the pH from 9.0 to 10.0 doubled the  
267 TAN flux from 62 to 115  $\text{g N}\cdot\text{m}^{-2}\cdot\text{day}^{-1}$ , while a less noticeable improvement was  
268 obtained when the pH was further increased to 11.0 (138  $\text{g N}\cdot\text{m}^{-2}\cdot\text{day}^{-1}$ ). The change in  
269 TAN flux at higher pH was also evident in the fitted  $K_m$  values, which sharply increased  
270 with pH. The fitted  $K_m$  values was slightly lower at pH 10.0 than at pH 11.0 with values  
271 of  $0.92\cdot 10^{-6}$  and  $1.13\cdot 10^{-6}$ , respectively. However, there was no significant difference in  
272  $K_m$  values when comparing 35 and 55 °C (Table 2). The superior performance of  $\text{NH}_3$   
273 membrane contactors at pH 10.0 and 11.0 is in accordance with the results reported  
274 by Ashrafizadeh and Khorasani (2010) and Noriega-Hevia et al. (2020), who reported a  
275  $K_m$  of  $10.9\cdot 10^{-6}$  and  $2.4\cdot 10^{-6} \text{ m}\cdot\text{s}^{-1}$  at pH 10, respectively. Vecino et al. (2019) and Reig et  
276 al. (2021) also reported similar  $K_m$  values when operating the same membrane module  
277 under similar conditions ( $0.7\cdot 10^{-6}$  and  $1\cdot 10^{-6} \text{ m}\cdot\text{s}^{-1}$ , respectively).  $\text{NH}_3$  diffusion through  
278 the membrane was not affected by the presence of acetic acid since similar  $K_m$  were  
279 observed for experiments carried out with and without acetic acid (data not shown).

280 This observation is in accordance with Daguerre-Martini et al. (2018), who assessed  
281 the effect of humic acids concentration in the feed solution on the TAN transfer using  
282 an e-PTFE membrane.

283 Acetic acid concentration in the feed solution remained constant during all the  
284 experiments at  $3.2 \text{ g COD}\cdot\text{L}^{-1}$  while its concentration in the trapping solution was below  
285 the detection limit for all experiments ( $<10 \text{ mg}\cdot\text{L}^{-1}$ ). These results are in line with the  
286 results of Molinuevo-Salces et al. (2018), who reported a minimal transfer of soluble  
287 organic matter ( $5\text{-}20 \text{ mg COD}\cdot\text{L}^{-1}\cdot\text{day}^{-1}$ ) and cations ( $0\text{-}20 \text{ mg}\cdot\text{L}^{-1}\cdot\text{day}^{-1}$ ) through an e-  
288 PTFE membrane when recovering TAN from pig manure. The retention of acetic acid  
289 allows hypothesising that VFAs with higher molecular weight (e.g., propionic acid,  
290 butyric acid) would not diffuse across the membrane and would not affect the nitrogen  
291 recovery efficiency under the tested operating conditions.

292 The specific reagent consumption ( $\text{mol reagent spent}\cdot\text{mol}^{-1} \text{ N recovered}$ ) after 8 hours  
293 was lower when working with higher feed pH values for both NaOH and  $\text{H}_2\text{SO}_4$  (Table  
294 2). These results show that the process is more reagent efficient at higher feed  
295 solution pH values. Reagent consumption during the test did not consider the reagents  
296 needed at the beginning of the process to reach the initial pH. Considering that only  
297  $\text{NH}_3$  was able to diffuse the membrane, the theoretical maximum consumption during  
298 the test would be  $1 \text{ mol NaOH}\cdot\text{mol}^{-1} \text{ N recovered}$  and  $0.5 \text{ mol H}_2\text{SO}_4\cdot\text{mol}^{-1} \text{ N recovered}$ .  
299 Since these experiments were performed using a synthetic solution without extra  
300 alkalinity, it is observed that the total reagents consumption approached to the  
301 theoretical value in those tests where a complete nitrogen recovery was obtained  
302 (e.g., Experiment 1F, 2E).

303 These experimental results allowed considering pH 10.0 as the preferable pH for this  
304 GPM contactor. In comparison with other pH values, pH 10.0 provides (i) a high TAN  
305 flux across the membrane and (ii) a lower consumption of reagents (alkali and acid) per  
306 unit of nitrogen recovered. This conclusion agrees with Ashrafizadeh and Khorasani  
307 (2010), who reported that pH above 10.7 did not improve  $\text{NH}_3$  removal. However, a  
308 recent study by Lee et al. (2021) suggested that the application of moderate alkaline  
309 pH values (i.e., 9.0) could be beneficial to prevent inorganic fouling on the membrane.

### 310 **3.2 OFMSW fermentation**

311 Figure 4 shows the VFAs, sCOD, TAN and pH values during OFMSW fermentation. The  
312 VFA concentration steadily increased from  $21.7 \text{ g COD}\cdot\text{L}^{-1}$  up to a maximum  
313 concentration of  $41.1 \text{ g COD}\cdot\text{L}^{-1}$  (day 7), with a concomitant pH decrease (from 6.96 to  
314 6.47). The VFA yield was  $0.63 \text{ g COD}_{\text{VFA}}\cdot\text{g}^{-1}$  VS, slightly higher than the fermentation  
315 yield reported by Fernandez-Domínguez et al. (2020), who fermented OFMSW from  
316 the same MBT plant. During the fermentation batch, the proportion of acetic and  
317 propionic acids remained nearly constant, while the proportion of valeric and caproic  
318 acids increased to the detriment of butyric acid (Figure 4a). At the end of the batch  
319 (day 8), the proportion of acetic, propionic, and butyric acids were 34%, 25% and 27%,  
320 respectively (Figure 4b). The  $\text{COD}_{\text{VFA}}/\text{sCOD}$  ratio increased over time reaching a final  
321 value of  $0.92\pm 0.05$  (Figure 4c). This  $\text{COD}_{\text{VFA}}/\text{sCOD}$  ratio is higher than the reported by  
322 Fernandez-Domínguez et al. (2020) but aligns with Valentino et al. (2021) results. The  
323 latter reported a  $\text{COD}_{\text{VFA}}/\text{sCOD}$  ratio of 0.90 when treating screw pressed OFMSW. The  
324 high acidification efficiency (percentage of sCOD as  $\text{COD}_{\text{VFA}}$ ) reached in this study is a



325 positive feature for the proposed biorefinery (Figure 1). On one hand, a fermentation  
326 broth with a low concentration of non-VFA soluble COD is preferable for PHA  
327 production, since it provides a good selection of PHA-storing microorganisms  
328 (Valentino et al., 2017). On the other hand, the low concentration of non-VFA sCOD  
329 implies that the organic matter that has not been converted to VFA is diverted to the  
330 anaerobic digester for biogas production. Finally, it is worth mentioning that the TAN  
331 concentration increased from 3.8 to 4.9 g·L<sup>-1</sup> due to ammonification of organic  
332 nitrogen (Figure 4d). The resulting TAN/COD<sub>VFA</sub> ratio is 0.12 mg N·mg<sup>-1</sup> COD, which is  
333 unfavourable to produce PHA (Sriyapai et al., 2021; Lee et al., 2014). Therefore,  
334 removing TAN from the fermentation broth is paramount to utilise this stream for PHA  
335 production.

### 336 **3.3 Ammonia recovery from the OFMSW fermentation liquid**

337 Figure 5 shows the TAN concentration evolution of the experiments carried out with  
338 the OFMSW fermentation liquid and Table 3 summarises their performance  
339 parameters. It can be observed that the operation time required to reach the same  
340 TAN recovery is much shorter than the time required for the synthetic fermentation  
341 liquid (Figure 3), which is attributed to the operation of the system at a higher area to  
342 volume ratio (membrane area to feed solution volume). The higher TAN fluxes  
343 obtained in these experiments compared to the ones obtained with the synthetic  
344 solution can be attributed to higher initial TAN concentration of the OFMSW  
345 fermentation liquid (higher concentration gradient).  $K_m$  will be the parameter used to  
346 compare these results with those obtained from the synthetic solution since it does

347 not depend on the operation time, the initial TAN concentration, nor the volumes of  
348 the feed and trapping solution as well as its ratio.

349 The  $K_m$  values obtained with the OFMSW fermentation liquid showed the same trend  
350 than those obtained with the synthetic solution: (i) a higher  $\text{NH}_3$  mass transfer at pH 10  
351 than at pH 9, and (ii) a higher  $\text{NH}_3$  mass transfer at 55 °C than at 35 °C. However, the  
352  $K_m$  values obtained using the OFMSW fermentation liquid were lower than those  
353 obtained with the synthetic solution. At 55 °C, the  $K_m$  values at pH 9.0 and 10.0 were  
354  $3.3 \cdot 10^{-7}$  and  $5.4 \cdot 10^{-7} \text{ m} \cdot \text{s}^{-1}$ , respectively, while the equivalent  $K_m$  for the synthetic  
355 solution were  $5.9 \cdot 10^{-7}$  and  $9.3 \cdot 10^{-7} \text{ m} \cdot \text{s}^{-1}$ . The lower performance of the GPM contactor  
356 using the OFMSW fermentation liquid cannot be attributed to membrane fouling since  
357 the tests conducted with the synthetic solution before and after operating the GPM  
358 with the OFMSW fermentation liquid reached the same  $K_m$  values (data not shown).  
359 The low membrane fouling observed in these experiments could be attributed to: (i)  
360 the low fouling propensity of PP membranes compared with other membranes such as  
361 PTFE membranes (Zarebska et al., 2015) and (ii) the low duration of the experiments (<  
362 8 h). Accordingly, the loss of performance could be related to the interference (e.g.,  
363 ionic interaction) of other species and the complex matrix of the fermentation liquid.  
364 As for the synthetic solution experiments, the specific reagent consumption per unit of  
365 TAN recovered was higher at pH 9 than at pH 10. The total NaOH and  $\text{H}_2\text{SO}_4$   
366 consumption in the OFMSW fermentation experiments was almost the same than the  
367 consumption in the synthetic feed experiments (Table 2 and 3). The NaOH required to  
368 adjust the pH at the beginning of the experiment was higher, but the amount of NaOH  
369 required to keep the pH at the set point was noticeably lower. This behaviour can be

370 explained by the alkalinity of the OFMSW fermentation liquid ( $9.1 \text{ g CaCO}_3 \cdot \text{L}^{-1}$ ) that  
371 acted as a buffer making the pH of the feed solution harder to raise, but also harder to  
372 decrease during the operation. The total consumption of  $\text{H}_2\text{SO}_4$  was similar to  
373 synthetic feed solution experiments, but its addition during the experiment was lower.  
374 It is worth noting that  $\text{H}_2\text{SO}_4$  consumption was slightly higher than the stoichiometric  
375 values of  $0.5 \text{ mol H}_2\text{SO}_4 \cdot \text{mol}^{-1} \text{ TAN}$  recovered, probably caused by the excess of acid in  
376 the trapping solution at the end of the test due to the limited accuracy of the dosing  
377 pump controlling the trapping solution pH. .

378 Figure 6 shows the VFA concentration during each experiment treating OFMSW  
379 fermentation liquid. The initial concentration was slightly lower ( $37.5\text{-}38.8 \text{ g COD}_{\text{VFA}} \cdot \text{L}^{-1}$   
380 <sup>1</sup>) than the measured at the end of the fermentation batch ( $41.1 \text{ g COD}_{\text{VFA}} \cdot \text{L}^{-1}$ ). This  
381 implies that a VFA loss occurred during sample post-treatment (i.e., filtration and  
382 centrifugation). During the experiments, none of the VFAs were detected in the  
383 trapping solution (detection limit of  $10 \text{ mg} \cdot \text{L}^{-1}$ ), which demonstrates that VFAs are  
384 unable to diffuse across the membrane under the tested conditions. However, a small  
385 VFA loss in the feed stream (8.7-10.7% on COD basis) was recorded during the  
386 experiments. The authors attribute this phenomenon to the biological aerobic  
387 degradation of these compounds. The feed tank was closed but it was not flushed and  
388 sealed with an inert gas (e.g.  $\text{N}_2$ ) to prevent the presence of oxygen. Strategies to  
389 minimize VFA losses should be considered in future research.

390 Finally, it is worth mentioning that no increase in ions concentration (i.e.,  $\text{Ca}^{2+}$ ,  $\text{Mg}^{2+}$ ,  
391  $\text{K}^+$ ,  $\text{Na}^+$ ,  $\text{Cl}^-$ ) was detected in the trapping solution (detection limit of  $0.5 \text{ mg} \cdot \text{L}^{-1}$ ).  
392 Similarly, the ions concentration in the feed solution at the beginning and at the end of

393 the experiments remained constant. Thus, it can be stated that ions did not diffuse  
394 through the membrane from the feed to the trapping solution, at least, at short-term  
395 conditions.

396 Overall, the results of these experiments show that the combination of acidogenic  
397 fermentation with a membrane contactor unit could be a technological solution to  
398 separate TAN and VFA.

### 399 **Conclusions**

400 A gas-permeable membrane contactor was used to recover ammoniacal nitrogen from  
401 fermentation broths. Nitrogen recovery efficiency improved at higher pH and  
402 temperatures. The optimum pH was 10 since high  $K_m$  were achieved at expenses of low  
403 reagent consumption. For the OFMSW fermentation liquid, the  $K_m$  values were lower  
404 than for the synthetic liquid, although the  $K_m$  followed the same trend with pH and  
405 temperature. Ions and VFA present in the fermentation liquid were not detected in the  
406 trapping solution. Overall, the results showed that membrane contactors can  
407 efficiently separate ammoniacal nitrogen and VFAs from fermentation broths.

### 408 **Supplementary material**

409 E-supplementary data for this work can be found in e-version of this paper online.

### 410 **Acknowledgements**

411 This work is supported by the project Ministry of Science, Innovation and Universities  
412 (PID2019-111284RB-I00) and the Water Research Institute of the University of  
413 Barcelona. S.A. is grateful to the Spanish Ministry of Science, Innovation and

414 Universities for his Ramon y Cajal fellowship (RYC-2017-22372). S.V. is grateful to the  
415 Generalitat de Catalunya for his predoctoral FI grant (2019 FI\_B 00394). A.S-T. also  
416 acknowledge the financial support of Indukern Company (Barcelona). F.M. and S.M.  
417 acknowledge the financial support from Generalitat de Catalunya (2017 SGR 1033) and  
418 Spanish Structures of Excellence María de Maeztu program through (MDM-2017-  
419 0767). Finally, the authors would like to thank the Catalan Government for the quality  
420 accreditation given to the Environmental Biotechnology research group of the  
421 University of Barcelona (2017 SGR 1218).

## 422 References

- 423 1. Ahn, Y.T., Hwang, Y.H., Shin, H.S., 2011. Application of PTFE membrane for  
424 ammonia removal in a membrane contactor. *Water Sci. & Technol.* 63.12. 2944-  
425 2948
- 426 2. Anthonisen, A.C., Loehr, R.C., Praskasam, T.B.S., Srinath, E.G., 1976. Inhibition of  
427 nitrification by ammonia and nitrous acid. *J. WPCF.* 48. 835-852.
- 428 3. APHA, Standard Methods for the Examination of Water and Wastewater, 23rd ed,  
429 2017. Water Environment Federation, Washington, D.C.
- 430 4. Ashrafizadeh, S.N., Khorasani, Z., 2010. Ammonia removal from aqueous solutions  
431 using hollow-fiber membrane contactors. *Chem. Eng. J.* 162. 1. 242-249.
- 432 5. Bayrakdar, A., Sürmeli, R.O., Çalli, B., 2017. Dry anaerobic digestion of chicken  
433 manure coupled with membrane separation of ammonia. *Biores. Technol.* 244. 1.  
434 816-823.
- 435 6. Boehler, M.A., Heisele, A., Seyfried, A., Grömping, M., Siegrist, H., 2015.  $(\text{NH}_4)_2\text{SO}_4$   
436 recovery from liquid side streams. *Envir. Sci. and Pollution Res.* 22. 7295–7305.

- 437 7. Bolzonella, D., Cavinato, C., Fatone, F., Pavan, P., Cecchi, F., 2012. High rate  
438 mesophilic, thermophilic, and temperature phased anaerobic digestion of waste  
439 activated sludge: A pilot scale study. *Waste Manage.* 32. 1196–1201.
- 440 8. Capson-Tojo, G., Moscoviz, R., Astals, S., Robles, A., Steyer, J.-P., 2020. Unraveling  
441 the literature chaos around free ammonia inhibition in anaerobic digestion.  
442 *Renewable and Sustainable Energy Rev.* 117. 109487.
- 443 9. Daguerre-Martini, S., Vanotti, M.B., Rodriguez-Pastor, M., Rosal, A., Moral, R.,  
444 2018. Nitrogen recovery from wastewater using gas-permeable membranes:  
445 Impact of inorganic carbon content and natural organic matter. *Water Res.* 137.  
446 201-210.
- 447 10. Darestani, M., Haigh, V., Couperthwaite, S.J., Millar, G.J., Nghiem, L.D., 2017.  
448 Hollow fibre membrane contactors for ammonia recovery: Current status and  
449 future developments. *J. of Envir. Chem. Eng.* 5. 1349-1359.
- 450 11. Dube, P.J. Vanotti, M.B., Szogi, A.A., García-González, M.C., 2016. Enhancing  
451 recovery of ammonia from swine manure anaerobic digester effluent using gas-  
452 permeable membrane technology. *Waste Manage.* 49. 372-377.
- 453 12. Fernández-Domínguez, D., Astals, S., Peces, M., Frison, N., Bolzonella, D., Mata-  
454 Alvarez, J., Dosta, J., 2020. Volatile fatty acids production from biowaste at  
455 mechanical-biological treatment plants: Focusing on fermentation temperature.  
456 *Biores. Technol.* 314. 123729.
- 457 13. Fillingham, M., Van der Zaag, A., Singh, J., Burt, S., Crolla, A., Kinsley, C.,  
458 MacDonald, D., 2017. Characterizing the performance of gas-permeable

- 459 membranes as an ammonia recovery strategy from anaerobically digested dairy  
460 manure. *Membranes*. 7. 4.
- 461 14. Frison, N., Katsou, E., Malamis, S., Oehmen, A., Fatone, F., 2015. Development of a  
462 novel process integrating the treatment of sludge reject water and the production  
463 of polyhydroxyalkanoates (PHAs). *Environ. Sci. Technol.* 49. 18. 10877–10885.
- 464 15. García-González, M., Vanotti, M., 2015. Recovery of ammonia from swine manure  
465 using gas-permeable membranes: Effect of waste strength and pH. *Waste Manag.*  
466 38. 455–461.
- 467 16. García-González, M., Vanotti, M., Szogi, A., 2015. Recovery of ammonia from swine  
468 manure using gas-permeable membranes: Effect of aeration. *J. of Envir. Manage.*  
469 152. 19-26.
- 470 17. González-García, I., Riaño, B., Molinuevo-Salces, B., Vanotti, M.B., García-González,  
471 M.C., 2021. Improved anaerobic digestion of swine manure by simultaneous  
472 ammonia recovery using gas-permeable membranes. *Water Res.* 190. 116789.
- 473 18. Lauterböck, B., Nikolausz, M., Lv, Z., Baumgartner, M., Liebhard, G., Fuchs, W.,  
474 2014. Improvement of anaerobic digestion performance by continuous nitrogen  
475 removal with a membrane contactor treating a substrate rich in ammonia and  
476 sulfide. *Biores. Technol.* 158. 209-216.
- 477 19. Lee, W.S., Chua, A.S.M., Yeoh, H.K., Ngoh, G.C., 2014. A review of the production  
478 and applications of waste-derived volatile fatty acids. *Chem. Eng. J.* 235. 83-99.
- 479 20. Lee, W., An, S., Choi, Y., 2021. Ammonia harvesting via membrane gas extraction at  
480 moderately alkaline pH: A step toward net-profitable nitrogen recovery from  
481 domestic wastewater. *Chem. Eng. J.* 405. 126662.

- 482 21. Lorini, L., di Re, F., Majone, M., Valentino, F., 2020. High-rate selection of PHA  
483 accumulating mixed cultures in sequencing batch reactors with uncoupled carbon  
484 and nitrogen feeding. *New Biotechnol.* 56. 140–148.
- 485 22. Menkveld, H.W.H., Broeders, E., 2018. Recovery of ammonia from digestate as  
486 fertilizer. *Water Practice and Technol.* 13. 382–387.
- 487 23. Micolucci, F., Gottardo, M., Bolzonella, D., Pavan, P., Majone, M., Valentino, F.,  
488 2020. Pilot-scale multi-purposes approach for volatile fatty acid production,  
489 hydrogen and methane from an automatic controlled anaerobic process. *J. of*  
490 *Cleaner Production.* 277. 124297.
- 491 24. Molinuevo-Salces, B., Riaño, B., Vanotti, M.B., García-González, M.C., 2018. Gas-  
492 permeable membrane technology coupled with anaerobic digestion for swine  
493 manure. *Frontiers in Sustainable Food Systems.* 2. Article 25.
- 494 25. Nagy, J., Kaljunen, J., Toth, A.J., 2019. Nitrogen recovery from wastewater  
495 and human urine with hydrophobic gas separation membrane: experiments  
496 and modelling. *Chem. Papers.* 73. 1903–1915.
- 497 26. Noriega-Hevia, G., Serralta, J., Borrás, L., Seco, A., Ferrer, J., 2020. Nitrogen  
498 recovery using a membrane contactor: Modelling nitrogen and pH evolution. *Envir.*  
499 *Chem. Eng. J.* 8. 103880.
- 500 27. Oliveira, C.S.S., Silva, C.E., Carvalho, G., Reis, M.A., 2017. Strategies for efficiently  
501 selecting PHA producing mixed microbial cultures using complex feedstocks: Feast  
502 and famine regime and uncoupled carbon and nitrogen availabilities. *New*  
503 *Biotechnol.* 37. 69-79.



- 504 28. Reig, M., Vecino, X., Gibert, O., Valderrama, C., Cortina, J.L., 2021. Study of the  
505 operational parameters in the hollow fibre liquid-liquid membrane contactors  
506 process for ammonia valorisation as liquid fertiliser. *Separation and Purification*  
507 *Technol.* 255. 117768.
- 508 29. Reis, M.A., Albuquerque, M., Villano, M., Majone, M., 2011. Mixed culture  
509 processes for Polyhydroxyalkanoate production from agro-industrial  
510 surplus/wastes as feedstocks. *Comprehensive Biotechnol.* (2nd Edit.). 6. 669-683.
- 511 30. Riaño, B., Molinuevo-Salces, B., Vanotti, M.B., García-González, M.C., 2019.  
512 Application of gas-permeable membranes for semi-continuous ammonia recovery  
513 from swine manure. *Environments.* 6.
- 514 31. Rongwong, W., Goh, K., 2020. Resource recovery from industrial wastewaters by  
515 hydrophobic membrane contactors: A review. *J. of Envir. Chem. Eng.* 104242.
- 516 32. Shi, X., Zuo, J., Zhang, M., Wang, Y., Yu, H., Li, B., 2019. Enhanced biogas production  
517 and in situ ammonia recovery from food waste using a gas-membrane absorption  
518 anaerobic reactor. *Biores. Technol.* 292. 121864.
- 519 33. Silva, F., Campanari, S., Matteo, S., Valentino, F., Majone, M., Villano, M., 2017.  
520 Impact of nitrogen feeding regulation on polyhydroxyalkanoates production by  
521 mixed microbial cultures. *New Biotechnol.* 37. Part A. 90-98.
- 522 34. Sriyapai, T., Chuarung, T., Kimbara, K., Samosorn, S., Sriyapai, P., 2021. Production  
523 and optimization of polyhydroxyalkanoates (PHAs) from *paraburkholderia* sp. PFN  
524 29 under submerged fermentation. *Electronic J. of Biotechnol.* Available online.

- 525 35. Valentino, F., Gianluca Munarin, G., Biasiolo, M., Cavinato, C., Bolzonella, D., Pavan,  
526 P., 2021. Enhancing volatile fatty acids (VFA) production from food waste in a two-  
527 phases pilot-scale anaerobic digestion process. *J. of Envir. Chem. Eng.* 9. 106062.
- 528 36. Valentino, F., Morgan-Sagastume, F., Campanaria, S., Villano, M., Werker, A.,  
529 Majone, M., 2017. Carbon recovery from wastewater through bioconversion into  
530 biodegradable polymers. *New Biotechnol.* 37. Part A. 9-23.
- 531 37. Vecino, X., Reig, M., Bhushan, B., Gibert, O., Valderrama, C., Cortina, J.L., 2019.  
532 Liquid fertilizer production by ammonia recovery from treated ammonia rich  
533 regenerated streams using liquid-liquid membrane contactors. *Chem. Eng. J.* 360.  
534 890-899.
- 535 38. Zarebska, A., Amor, A.C., Ciurkot, K., Karring, H., Thygesen, O., Andersen, T.P.,  
536 Hägg, M-B., Christensen, K.V., Norddahl, B., 2015. Fouling mitigation in membrane  
537 distillation processes during ammonia stripping from pig manure. *J. of Mem. Sci.*  
538 484, 119-132.

#### 539 **Authors contribution statement**

540 **Andreu Serra-Toro:** Methodology, Investigation, Formal analysis, Writing - original draft,  
541 Visualisation. **Sergi Vinardell:** Methodology, Writing - review & editing, Visualisation.  
542 **Sergi Astals:** Conceptualization, Writing - Review & Editing, Supervision, Visualisation,  
543 Funding acquisition. **Sergio Madurga:** Formal analysis, Writing - Review & Editing,  
544 Visualisation, **Joan Llorens:** Methodology, Writing - Review & Editing. **Joan Mata-**  
545 **Álvarez:** Writing - Review & Editing, Funding acquisition. **Francesc Mas:**  
546 Conceptualization, Methodology, Formal analysis, Writing - Review & Editing,  
547 Supervision, Visualisation, Funding acquisition. **Joan Dosta:** Conceptualization,

548 Methodology, Investigation, Writing - Review & Editing, Supervision, Visualisation,

549 Funding acquisition.

550 39.

551 **Declaration of interests**

552

553  The authors declare that they have no known competing financial interests or personal  
554 relationships that could have appeared to influence the work reported in this paper.

555

556  The authors declare the following financial interests/personal relationships which may be  
557 considered as potential competing interests:

558

Andreu Serra-Toro reports financial support was provided by Indukern company  
(Barcelona).

559

560 40.

561 **Highlights**

562 - Membrane contactor efficiently recovered  $\text{NH}_3$  from a biowaste fermentation broth

563

564 - Membrane contactor allowed a complete separation of  $\text{NH}_3$  from volatile fatty acids

565

566 - Higher operating temperatures and pH enhanced  $\text{NH}_3$  mass transfer rate

567

568 -  $\text{NH}_3$  was successfully recovered at alkaline pHs (9, 10 and 11) at 35 and 55 °C

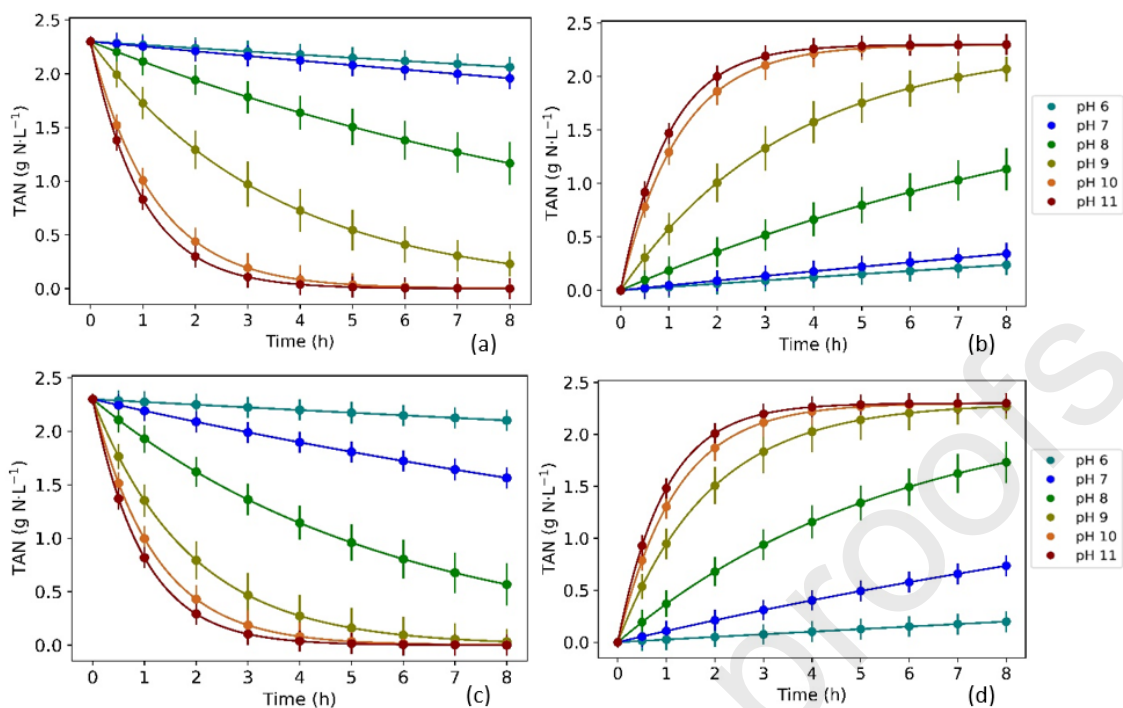
569

570 - Ions present in the fermentation broth were not detected in the trapping solution

571

572 41.

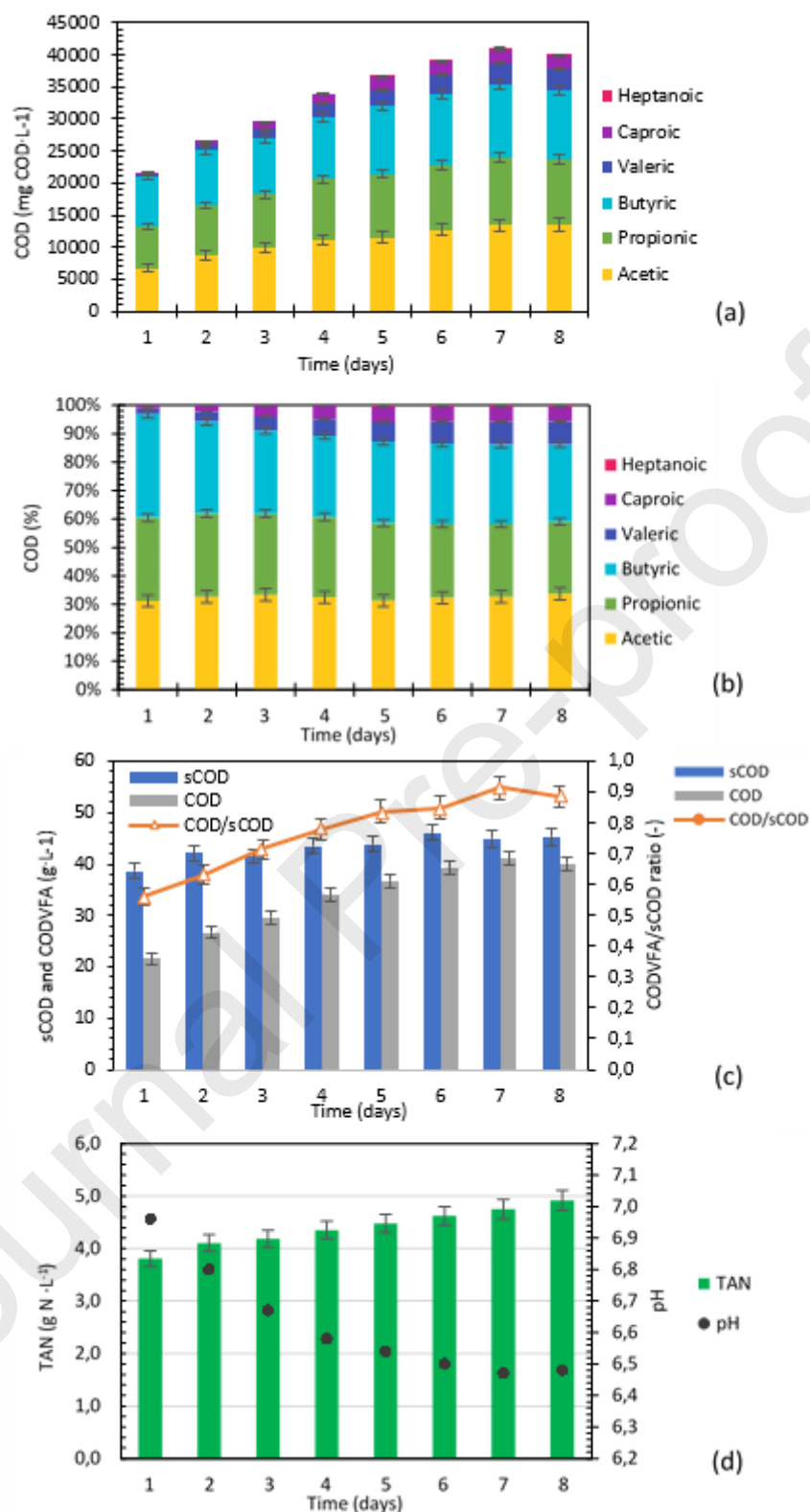




580

581 **Figure 3.** Experimental (dots) and modelled (solid lines) TAN concentration over time at  
 582 different synthetic solution pH and temperature. (top) experiments at 35 °C (a) feed solution  
 583 and (b) trapping solution, and (bottom) experiments at 55 °C (c) feed solution and (d) trapping  
 584 solution. Error bars represent the standard deviation.

585 44.

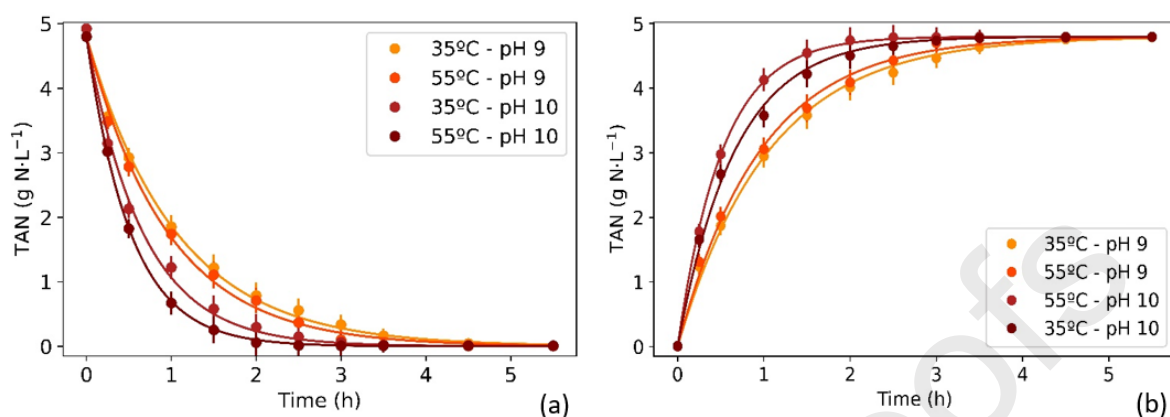


586

587 **Figure 4.** OFMSW fermentation performance, (a) VFA concentration, (b) proportion of the VFA,  
 588 (c) concentration of COD<sub>VFA</sub>, sCOD and its ratio, (d) concentration of TAN and pH. Error bars  
 589 represent the standard deviation.

590

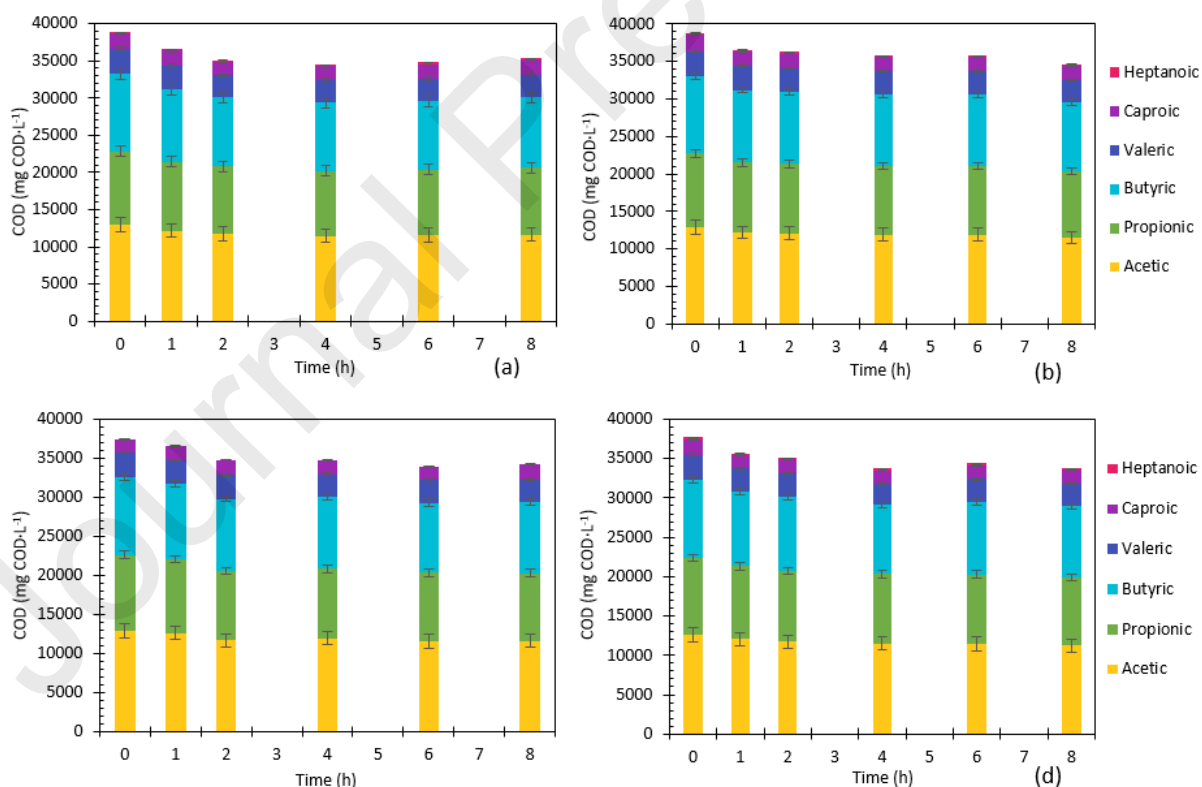
591 45.



592

593 **Figure 5.** TAN concentration evolution of the (a) feed solution and (b) trapping solution for the  
 594 experiments carried out with OFMSW fermentation liquid. Error bars represent standard  
 595 deviation.

596 46.



597

598 **Figure 6.** Evolution of the VFA concentration in the feed solution for experiments (a) 3A at pH  
 599 9.0 and 35 °C, (b) 3B at pH 9.0 and 55 °C, (c) 3C at pH 10.0 and 35 °C and (d) 3D at pH 10.0 and  
 600 55 °C. Error bars represent the standard deviation.

601 47.

602

**Table 1.** Operational conditions of the experiments carried out in this study.

Feed solution	Test	Feed solution pH (-)	Temperature (°C)
Synthetic fermentation liquid	1A	6.0	35
	1B	7.0	35
	1C	8.0	35
	1D	9.0	35
	1E	10.0	35
	1F	11.0	35
	2A	6.0	55
	2B	7.0	55
	2C	8.0	55
	2D	9.0	55
	2E	10.0	55
	2F	11.0	55
OFMSW fermentation liquid	3A	9.0	35
	3B	10.0	35
	3C	9.0	55
	3D	10.0	55

603

604 48.

605

**Table 2.** Operational conditions and performance parameters in experiments using synthetic fermentation liquid (average values  $\pm$  standard deviation).

606

Exp.	T °C	pH -	TAN recovery at 8h %	Average flux at 8h g N·day <sup>-1</sup> ·m <sup>-2</sup>	K <sub>m</sub> m·s <sup>-1</sup>	Alkali consumption		Acid consumption	
						Total*	Test**	Total*	Test**
1A	35	6.0	8	2.5 $\pm$ 0.3	(2.2 $\pm$ 0.5)·10 <sup>-8</sup>	4.5 $\pm$ 0.5	0.64 $\pm$ 0.06	2.32 $\pm$ 0.27	1.03 $\pm$ 0.10
1B		7.0	16	4.3 $\pm$ 0.6	(2.8 $\pm$ 0.4)·10 <sup>-8</sup>	2.5 $\pm$ 0.3	0.60 $\pm$ 0.06	2.14 $\pm$ 0.25	1.14 $\pm$ 0.11
1C		8.0	65	17 $\pm$ 3	(9.5 $\pm$ 1.3)·10 <sup>-8</sup>	1.4 $\pm$ 0.1	0.64 $\pm$ 0.06	0.87 $\pm$ 0.09	0.64 $\pm$ 0.07
1D		9.0	91	62 $\pm$ 10	(3.2 $\pm$ 0.3)·10 <sup>-7</sup>	1.0 $\pm$ 0.1	0.55 $\pm$ 0.06	0.63 $\pm$ 0.07	0.52 $\pm$ 0.06
1E		10.0	100	115 $\pm$ 16	(9.2 $\pm$ 0.4)·10 <sup>-7</sup>	1.0 $\pm$ 0.1	0.12 $\pm$ 0.03	0.61 $\pm$ 0.07	0.52 $\pm$ 0.06
1F		11.0	100	138 $\pm$ 17	(1.13 $\pm$ 0.03)·10 <sup>-6</sup>	1.1 $\pm$ 0.1	0.02 $\pm$ 0.01	0.61 $\pm$ 0.07	0.50 $\pm$ 0.05
2A	55	6.0	10	2.8 $\pm$ 0.3	(1.3 $\pm$ 0.3)·10 <sup>-8</sup>	4.1 $\pm$ 0.5	0.65 $\pm$ 0.06	2.41 $\pm$ 0.25	1.15 $\pm$ 0.12
2B		7.0	36	10 $\pm$ 2	(5.8 $\pm$ 1.0)·10 <sup>-8</sup>	1.8 $\pm$ 0.2	0.69 $\pm$ 0.06	0.95 $\pm$ 0.11	0.61 $\pm$ 0.07
2C		8.0	73	32 $\pm$ 5	(1.9 $\pm$ 0.1)·10 <sup>-7</sup>	1.2 $\pm$ 0.1	0.68 $\pm$ 0.06	0.67 $\pm$ 0.08	0.56 $\pm$ 0.07
2D		9.0	99	84 $\pm$ 11	(5.9 $\pm$ 0.5)·10 <sup>-7</sup>	1.2 $\pm$ 0.1	0.33 $\pm$ 0.04	0.65 $\pm$ 0.09	0.54 $\pm$ 0.06
2E		10.0	100	121 $\pm$ 16	(9.3 $\pm$ 0.3)·10 <sup>-7</sup>	1.2 $\pm$ 0.1	0.18 $\pm$ 0.02	0.50 $\pm$ 0.04	0.48 $\pm$ 0.05
2F		11.0	100	133 $\pm$ 16	(1.15 $\pm$ 0.04)·10 <sup>-6</sup>	1.1 $\pm$ 0.1	0.00 $\pm$ 0.00	0.63 $\pm$ 0.04	0.52 $\pm$ 0.05

607 \* NaOH and H<sub>2</sub>SO<sub>4</sub> including the initial reagent consumption and the consumption during the experiment608 \*\* NaOH and H<sub>2</sub>SO<sub>4</sub> consumption during the experiment to keep the pH at the set point.

609

49.



610 **Table 3. Operational characteristics and results obtained in experiments using OFMSW**  
 611 **fermentation broth as feed solution (average values  $\pm$  standard deviation).**

Exp.	T °C	pH	TAN recovery at 8h %	Average flux at 8h g N·day <sup>-1</sup> ·m <sup>-2</sup>	K <sub>m</sub> m·s <sup>-1</sup>	Alkali consumption		Acid consumption	
						mol NaOH·mol <sup>-1</sup> TAN recovered		mol H <sub>2</sub> SO <sub>4</sub> ·mol <sup>-1</sup> TAN recovered	
						Total*	Test**	Total*	Test**
3A	35	9.0	100	78.4 $\pm$ 11.0	(2.8 $\pm$ 6.0)·10 <sup>-7</sup>	1.02 $\pm$ 0.10	0.25 $\pm$ 0.04	0.63 $\pm$ 0.06	0.25 $\pm$ 0.03
3B		10.0	100	120.1 $\pm$ 14.4	(5.0 $\pm$ 9.2)·10 <sup>-7</sup>	0.94 $\pm$ 0.10	0.10 $\pm$ 0.02	0.65 $\pm$ 0.06	0.14 $\pm$ 0.02
3C	55	9.0	100	91.0 $\pm$ 12.7	(3.3 $\pm$ 6.3)·10 <sup>-7</sup>	0.97 $\pm$ 0.11	0.21 $\pm$ 0.03	0.67 $\pm$ 0.07	0.21 $\pm$ 0.03
3D		10.0	100	138.8 $\pm$ 16.7	(5.4 $\pm$ 5.7)·10 <sup>-7</sup>	0.86 $\pm$ 0.08	0.05 $\pm$ 0.02	0.63 $\pm$ 0.06	0.17 $\pm$ 0.02

612 \* NaOH and H<sub>2</sub>SO<sub>4</sub> including the initial reagent consumption and the consumption during the experiment

613 \*\* NaOH and H<sub>2</sub>SO<sub>4</sub> consumption during the experiment to keep the pH at the set point.

614 50.